Pergamon

Int. J. Multiphase Flow Vol. 24, No. 1, pp. 131–143, 1998

Printed in Great Britain

PII: S0301-9322(97)00036-0

0301-9322/98 $19.00 + 0.00

WALL-TRIGGERED INTERFACIAL RESONANCE IN LAMINAR GAS–LIQUID FLOW

V. BONTOZOGLOU and G. PAPAPOLYMEROU

Department of Mechanical & Industrial Engineering, University of Thessaly, Pedion Areos, GR-38334 Volos, Greece

(Received 15 August 1996; in revised form 29 April 1997)

Abstract—Laminar gas–liquid flow through a channel with corrugated bottom, driven by a combination of gravity and pressure drop, is considered. A linear analysis, valid for small-amplitude disturbances but arbitrary wavelength and Re number, leads to Orr–Sommerfeld type equations with nonhomogeneous boundary conditions. The interface amplitude relative to the wall is examined and linearly infinite amplification is computed at specific resonance conditions. With increasing gas velocity, the range of corrugation wavelengths most active in producing strong interaction with the interface expands considerably, and moves to higher values. It is argued that the resonant phenomenon under consideration may influence the interfacial dynamics of gas–liquid flows in small-scale passages. © 1997 Published by Elsevier Science Ltd

Key Words: gas–liquid separated flow, wall corrugations, linear analysis, interfacial resonance

1. INTRODUCTION

Flows bounded by a wall with small-amplitude perturbations comprise an interesting class of problems with periodic forcing. Such flows are in principle liable to resonance phenomena in the neighbourhood of their characteristic frequencies. The case presently under investigation is the separated (co- or countercurrent) flow of a gas and a liquid through a channel with corrugated top and bottom walls.

This setup is a useful prototype of the periodic flow constrictions appearing in the small passage of process equipment such as absorption columns, and trickle-bed reactors. Also, surface modifications of condensers and falling-film evaporators—aimed at increasing heat transfer rates—are frequently of a similar geometry.

Of special interest is a consideration of the effect of gas-shear, under conditions such that it is not negligible. Indeed, during gas–liquid flow away from flooding, gas-shear is often neglected and the flow is modelled as a liquid film driven solely by gravity.

The effect of linear wall perturbations in such zero-shear flow has been studied in previous work (Bontozoglou & Papapolymerou 1996). The main conclusion was that a moderate amplification of the wall structure (with maximum value approaching 2.5) occurs for wavelengths in the range 0.001 to 0.005 m and Re = 100–300. This falling film behaviour was associated with a resonance phenomenon involving inertial terms, as indicated by the fact that it was not observed in previous analytical and numerical calculations based on the Stokes approximation (Wang 1981, Pozrikidis 1988).

The only other prediction of such a resonance known to the authors appears in the inviscid theory of uniform, horizontal flow over a wavy wall (Kennedy 1963, Mei 1969, Miles 1986, Bontozoglou *et al.* 1991, Sammarco *et al.* 1994). Linear inviscid theory predicts that for a uniform liquid velocity U equal to

$$U^2 = (g/k)\tanh kh \qquad [1]$$

resonance takes place between a stationary surface wave and the bottom forcing, leading to infinite free-surface amplitude. Symbols h and k in [1] denote liquid film thickness and wave number of the wall corrugations respectively. This theory is realistic for large-scale phenomena (sediment transport in rivers, Bragg scattering of ocean waves in harbours) and only for horizontal or near-horizontal flows.

The falling film, viscous resonance reported by Bontozoglou and Papapolymerou (1996) manifests itself for short wall corrugations and very thin films. Because of the small scale, the restoring force is surface tension rather than gravity, and the phenomenon appears for flow at any inclination from vertical to horizontal. However, the linear amplification computed is finite, leaving the practical significance of the phenomenon open to question.

The goal of the present work is to investigate the effect of a parallel gas flow (co- or counter-current) on this resonance. Two-phase flow with a similar geometry has only been considered in the limit of zero Re number (Dassori *et al.* 1984), where again the wall flow resonance does not appear. With the inclusion of inertia terms, it is intuitively expected that the moving gas will exert a destabilizing influence. Two known mechanisms—caused by the periodic variation of interfacial pressure and shear stress—are the wave crest suction by a Bernoulli effect and the energy input by work done on the interface (Hanratty 1983). (In the context of the present study, we do not refer to instability in the classical sense, but rather to steady configurations corresponding to high interfacial wave amplitude.)

The analysis is based on the assumption of wall corrugations with amplitude a much smaller than the liquid film height h. Flow variables are expanded with respect to the small parameters $\varepsilon = a/h$ and the linear, first-order problem is solved numerically by a finite-difference scheme.

2. FORMULATION OF THE PROBLEM

Two-dimensional flow is considered through a channel at an angle ϕ relative to the vertical direction. The channel bottom wall is covered with small-amplitude sinusoidal corrugations at right angles to the flow direction (figure 1). The flow is described by an x, y coordinate system,

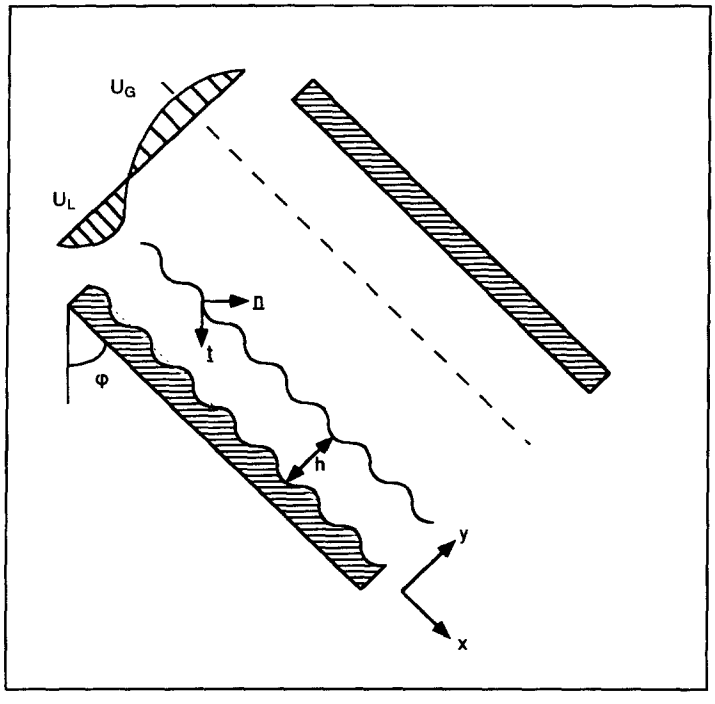

Figure 1. Sketch of the flow with all pertinent parameters.

where y is the direction pointing away from the wavy wall. The origin of the y-axis is set at the mean lower wall level and the corrugations are described by the equation

$$w(x) = a \cos kx \quad [2]$$

The computational domain extends from the corrugated wall to the zero-shear plane in the gas flow. Thus, details of the gas flow near the upper wall, which are not of immediate interest to the present study, are not computed.

The mean liquid film thickness is equal to h and the free surface of the liquid is located at

$$\eta(x) = h + f(x) \quad [3]$$

The interface shape $f(x)$ is described by the linear relation

$$f(x) = \beta a \, e^{ikx} \quad [4]$$

where β is the amplification of the wall corrugations and is in general complex. This expression corresponds to waves of the same wavelength as the disturbances but of arbitrary amplitude and phase relative to the wall. The mean thickness of the gas phase, up to the zero-shear plane, is equal to m. Thus, the average width of the computational domain is

$$W = h + m \quad [5]$$

The flow in each fluid domain is described by the continuity equation and the two components of the Navier–Stokes equation. Subscripts L and G are used to denote the liquid and gas phase variables. Boundary conditions are no-slip on the solid wall:

$$u_L = v_L = 0 \quad \text{on } y = w(x) \quad [6]$$

Also, the velocity normal to the stationary interface is zero for each phase

$$\mathbf{u}_L \cdot \mathbf{n} = 0 \quad [7a]$$

$$\mathbf{u}_G \cdot \mathbf{n} = 0 \quad \text{on } y = \eta(x) \quad [7b]$$

where $\mathbf{u} = (u, v)$. Terms $\mathbf{n}$ and $\mathbf{t}$ are the unit vectors, locally normal and tangential to the interface, and are given (in terms of the interface slope f') by the expressions

$$\mathbf{t} = (1, f')/\sqrt{1 + f'^2} \quad [8a]$$

$$\mathbf{n} = (f', -1)/\sqrt{1 + f'^2} \quad [8b]$$

(Note that, throughout the text, derivatives are denoted by primes and subscripts are used to define the phase or the directional component.)

Continuity of velocities along the interface dictates the condition

$$\mathbf{u}_L \cdot \mathbf{t} = \mathbf{u}_G \cdot \mathbf{t} \quad \text{on } y = \eta(x) \quad [9]$$

Shear and normal stresses balance on the interface, giving the equations

$$(\underline{\boldsymbol{\sigma}}_L \cdot \mathbf{n}) \cdot \mathbf{t} = (\underline{\boldsymbol{\sigma}}_G \cdot \mathbf{n}) \cdot \mathbf{t} \quad [10]$$

$$(\underline{\boldsymbol{\sigma}}_L \cdot \mathbf{n}) \cdot \mathbf{n} - (\underline{\boldsymbol{\sigma}}_G \cdot \mathbf{n}) \cdot \mathbf{n} = s \frac{f''}{(1 + f'^2)^{3/2}} \quad [11]$$

Symbol s denotes the surface tension and $\underline{\boldsymbol{\sigma}}$ is the stress tensor, defined for each fluid in terms of the rate of strain tensor $\underline{\mathbf{e}}$ and Kronecker $\underline{\boldsymbol{\delta}}$ as:

$$\underline{\boldsymbol{\sigma}} = -p\underline{\boldsymbol{\delta}} + 2\mu\underline{\mathbf{e}} \quad [12]$$

Finally, at the zero-stress plane, the slope of the gas velocity profile is set equal to zero, resulting in the condition

$$du_G/dy = 0 \quad \text{on } y = h + m \quad [13]$$

The perturbation expansion performed is based on the small variable ε defined as

$$\varepsilon = a/h \quad [14]$$

The flow is described by the stream functions, ψ_L and $\Psi^{(G)}$, which are expanded perturbation series in the small variable ε:

$$\psi_L = \psi_L^{(0)} + \varepsilon\psi_L^{(1)} \quad [15a]$$

$$\psi_G = \psi_G^{(0)} + \varepsilon\psi_G^{(1)} \quad [15b]$$

The zero-order problem corresponds to laminar flow in a channel with flat walls. The flow is driven by a combination of gravity in the direction of flow, g_x, and pressure drop, $\Delta P/L$. We define the terms

$$p_L = \frac{1}{\nu_L}\left(\frac{\Delta P/L}{\rho_L} - g_x\right) \quad [16a]$$

$$p_G = \frac{1}{\nu_G}\left(\frac{\Delta P/L}{\rho_G} - g_x\right) \quad [16b]$$

where ρ and ν are the density and kinematic viscosity of the two phases. After algebraic manipulations, the following solution is derived:

$$\psi_L^{(0)} = \frac{p_L y^3}{6} + \frac{Ay^2}{2} \quad [17a]$$

$$\psi_G^{(0)} = \frac{p_g y^3}{6} + \frac{By^2}{2} + Cy \quad [17b]$$

where

$$A = -p_G(h+m)\left(\frac{\rho_G}{\rho_L}\right)\left(\frac{\nu_G}{\nu_L}\right) + \frac{g_x h}{\nu_L}\left(1 - \frac{\rho_G}{\rho_L}\right) \quad [18a]$$

$$B = -p_G(h+m) \quad [18b]$$

$$C = (p_L - p_G)\frac{h^2}{2} + h(A - B) \quad [18c]$$

When $\Delta P/L$ is opposite to the direction of gravity, gas shear pulls the liquid upward. Representative velocity profiles with increasing gas velocity, shown in figure 2, have the expected gradual transition from countercurrent to cocurrent flow.

The first-order problem is treated by following the linear response of [4]. The respective stream function terms are expressed as

$$\psi_L^{(1)}(x, y) = \psi_L(y)\, e^{ikx} \quad [19a]$$

$$\psi_G^{(1)}(x, y) = \psi_G(y)\, e^{ikx} \quad [19b]$$

Modelling of the gas-phase disturbance by [19b] implies that separation above the waves does not take place, which is consistent with the linear approximation adopted throughout the study.

[19a & b] are substituted in the Navier–Stokes equations for each phase, which are subsequently combined to eliminate the pressure and lead to Orr–Sommerfeld type ordinary differential equations. The variables are non-dimensionalized by using the mean liquid film thickness h as the characteristic length for both phases, the volume flow rates per unit span, q_L and q_G, as the characteristic values for the stream functions, and q_L/h and q_G/m as the characteristic velocities. The resulting dimensionless equations are

$$\left(\frac{1}{ik\ \mathrm{Re}_L}\right)(D^2 - k^2)^2\psi_L = U_L(D^2 - k^2)\psi_L - U_L''\psi_L \quad [20a]$$

$$\left(\frac{1}{ik\ \mathrm{Re}_G}\right)(D^2 - k^2)^2\psi_G = \frac{h}{m}\left\{U_G(D^2 - k^2)\psi_G - U_G''\psi_G\right\} \quad [20b]$$

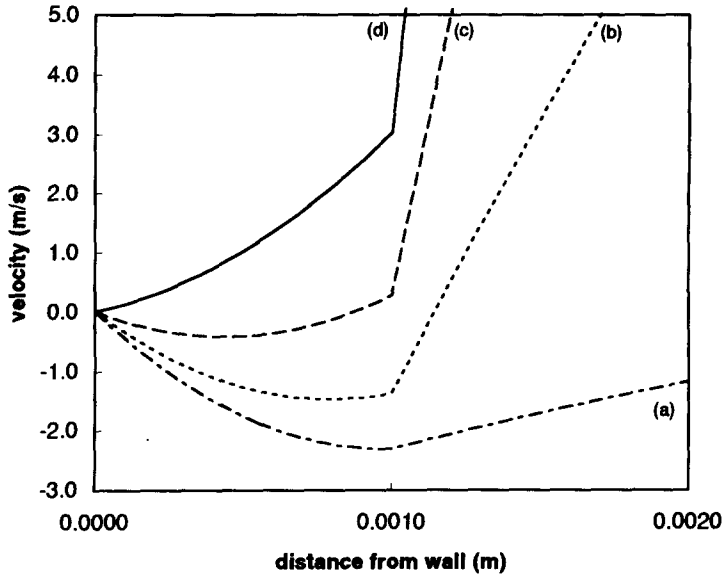

Figure 2. Zero-order velocity profiles in the liquid film and around the interface for film thickness $h = 0.001$ m and $\Delta P/L = 30$, 200, 500 and 100 N/m^3 (a to d respectively).

where $\mathrm{Re_L}$ and $\mathrm{Re_G}$ are the two Reynolds numbers, defined as

$$\mathrm{Re_L} = \frac{q_L}{\nu_L} \qquad [21a]$$

$$\mathrm{Re_G} = \frac{q_G}{\nu_G} \qquad [21b]$$

Term D is the differential operator d/dy and U_L, U_G are the dimensionless, zero-order velocities, given by the expressions

$$U_L = \left(\frac{h}{q_L}\right)\left(\frac{p_L h^2 y^2}{2} + Ahy\right) \qquad [22a]$$

$$U_G = \left(\frac{m}{q_G}\right)\left(\frac{p_G h^2 y^2}{2} + Bhy + C\right) \qquad [22b]$$

For conciseness, the same symbols are retained for the now dimensionless variables y, D, k, ψ_L, ψ_G, U_L and U_G.

[20] is the familiar Orr–Sommerfeld equation of linear stability without the phase velocity parameter. However, the present problem is not an eigenvalue problem, since not all boundary conditions are homogeneous.

According to a well-known technique, the dimensionless boundary conditions along the wall and the interface are expanded in Taylor series around the respective mean levels ($y = 0$ and $y = 1$). The final expressions are

$$\psi_L(0) = 0 \qquad [23a]$$

$$\psi_L'(0) = -U_L'(0) \qquad [23b]$$

$$\psi_L(1) = -\beta U_L(1) \qquad [23c]$$

$$\psi_G(1) = -\beta\left(\frac{h}{m}\right)U_G(1) \qquad [23d]$$

$$\beta U_L'(1) + \psi_L'(1) = \left(\frac{q_G}{q_L}\right)\{\beta U_G'(1) + \psi_G'(1)\} \quad [23e]$$

$$\psi_L''(1) + k^2\psi_L(1) + \beta U_L''(1) = \left(\frac{\mu_G}{\mu_L}\right)\left(\frac{q_G}{q_L}\right)\left\{\psi_G''(1) + k^2\psi_G(1) + \beta\left(\frac{h}{m}\right)U_G''(1)\right\} \quad [23f]$$

$$\left(\frac{\mu_G}{\mu_L}\right)\left(\frac{q_G}{q_L}\right)\left\{3ik\psi_G'(1) - \frac{i}{k}\psi_G'''(1) - \left(\frac{h}{m}\right)\mathrm{Re}_G U_G\psi_G'(1)\right\} + \left\{3ik\psi_L'(1) - \frac{i}{k}\psi_L'''(1) - \mathrm{Re}_L U_L\psi_L'(1)\right\}$$

$$= -\left(\frac{\beta}{q_L\mu_L}\right)\{sk^2h + (\rho_L - \rho_G)g_z h^3\} - \beta\,\mathrm{Re}_L U_L(1)U_L'(1) + \beta\left(\frac{\mu_G}{\mu_L}\right)\left(\frac{q_G}{q_L}\right)\left(\frac{h}{m}\right)^2\mathrm{Re}_G U_G(1)U_G'(1) \quad [23g]$$

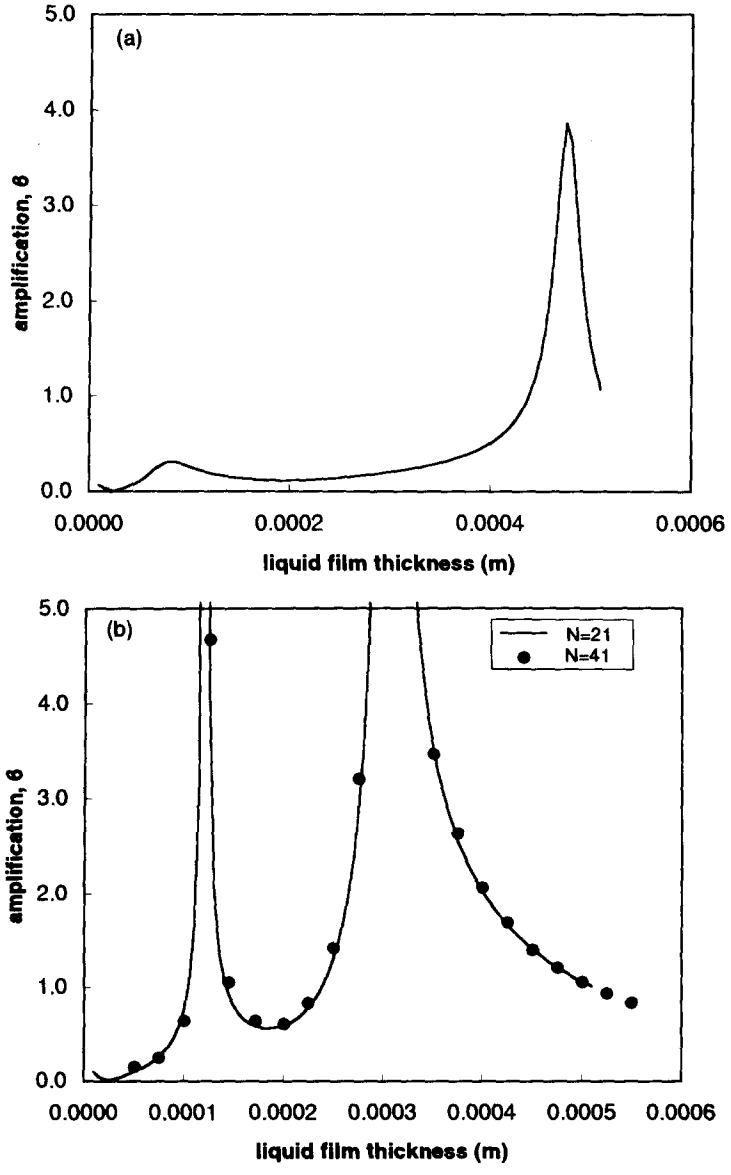

Fig. 3(a,b)

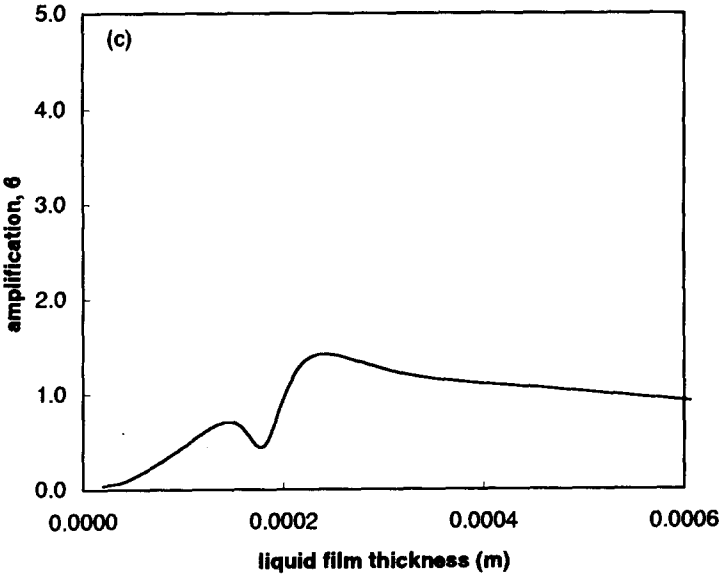

Figure 3. The interfacial amplification as a function of liquid film thickness, for gas spacing $m = 0.005$ m and pressure drop $\Delta P/L = 30$ N/m^3. Plots refer to wall corrugations with the following length: (a) 0.0025 m, (b) 0.005 m, (c) 0.01 m. The points in (b) are computed with a finer discretization $N_L = N_G = 41$.

Finally, the condition along the zero-shear plane results in the equations

$$\psi_G\left(1 + \frac{m}{h}\right) = 0 \qquad [24a]$$

$$\psi_G''\left(1 + \frac{m}{h}\right) = 0 \qquad [24b]$$

3. NUMERICAL SOLUTION

[20a & b] with the boundary conditions [23a–f] and [24a & b] are solved by a centred, finite-difference scheme. The liquid and gas film are discretized by N_L and N_G equally spaced points respectively. At each point, the value of the unknown stream function amplitude, ψ_L or ψ_G, is split into a real and an imaginary part. Eight additional (fictitious) points—two on each side of each region—are added to discretize the third and fourth derivatives. The last two unknowns are the real and imaginary parts of the free surface amplitude β. Thus, the total number of unknowns is $2(N_L + 4) + (2N_G + 4) + 2 = 2N_L + 2N_G + 18$.

[20a & b] are applied to the N_L and N_G points across the liquid and gas film respectively, resulting in $N_L + N_G$ equations. The boundary conditions provide another nine complex equations. Setting the real and imaginary parts to zero leads to $(2N_L + 2N_G + 18)$ linear algebraic equations in the unknowns.

Test runs were performed with N_L and N_G taking the values 11, 21 and 41. The results presented are computed using $N_L = N_G = 21$. This discretization proved accurate enough for the purposes of the present study, as indicated by figure 3(b), where representative points (computed with $N_L = N_G = 41$) coincide with the rest of the results.

4. RESULTS

Computations are done for liquid and gas with kinematic viscosities $\nu_L = 10^{-6}$ m^2/s and $\nu_G = 10^{-4}$ m^2/s respectively. The range of Re_L and Re_G numbers covered is such that the laminar solution is expected to offer realistic estimates. It may be argued that for a range of the Re numbers

considered, the interface will be wavy because of the growth of linearly unstable disturbances independent of the corrugated walls. However, in the linear approximation the two phenomena are separable. Therefore, the present analysis is valid and the final flow is the result of linear superposition. The coupling of free and forced oscillations *in the non-linear regime* is a very interesting question which is beyond the scope of the present work.

The main variable examined is the dimensionless interfacial amplitude β, as a function of flow parameters and wavelength of the sinusoidal wall corrugations. Different inclinations were tested and representative results are shown for a channel at an angle $\phi = 60^\circ$ to the vertical and also for a horizontal channel. In the calculations, the pressure drop $\Delta P/L$ and void fraction h are taken as input parameters and liquid and gas flow rates are computed from the zero-order solution. Pressure drop is always in the direction forcing the gas to flow upward.

In the limit of $Re_L = 0$, $Re_G = 0$, the results of Dassori *et al.* (1984) are recovered. There are an extension of the free-surface results of Wang (1981), with no major qualitative differences.

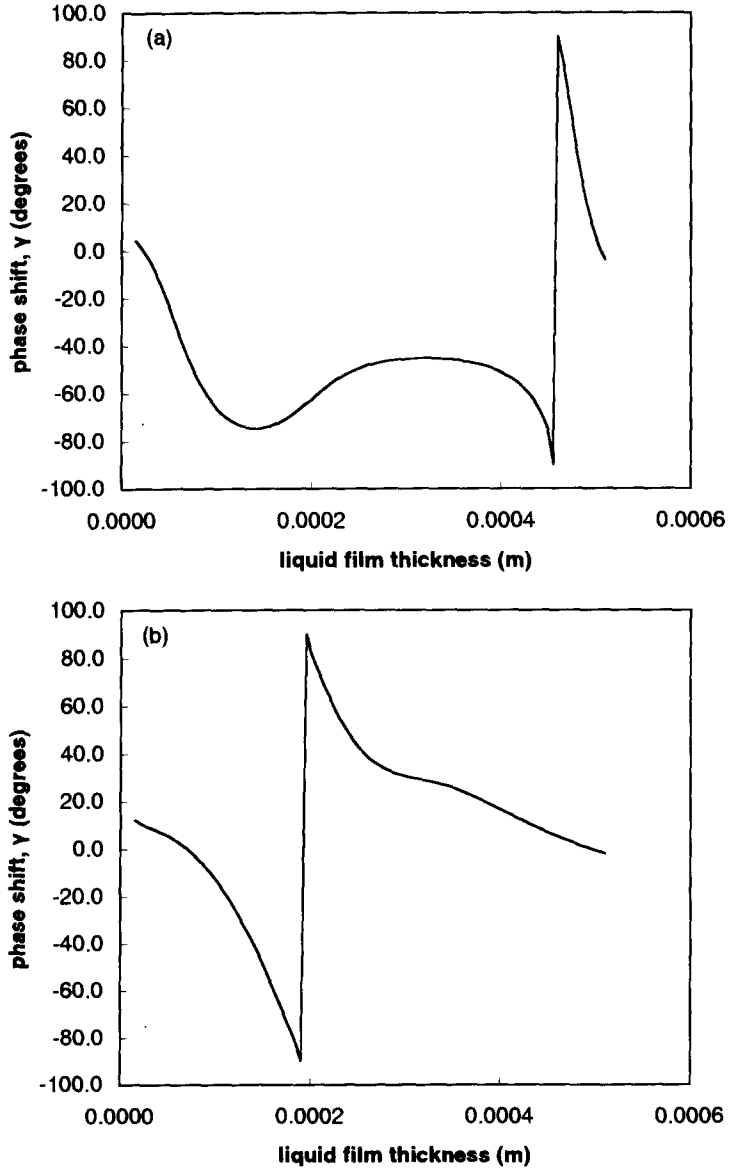

Figure 4. The phase of the interface relative to the wall as a function of liquid film thickness for wavelengths (a) $L = 0.0025$ m and (b) $L = 0.005$ m.

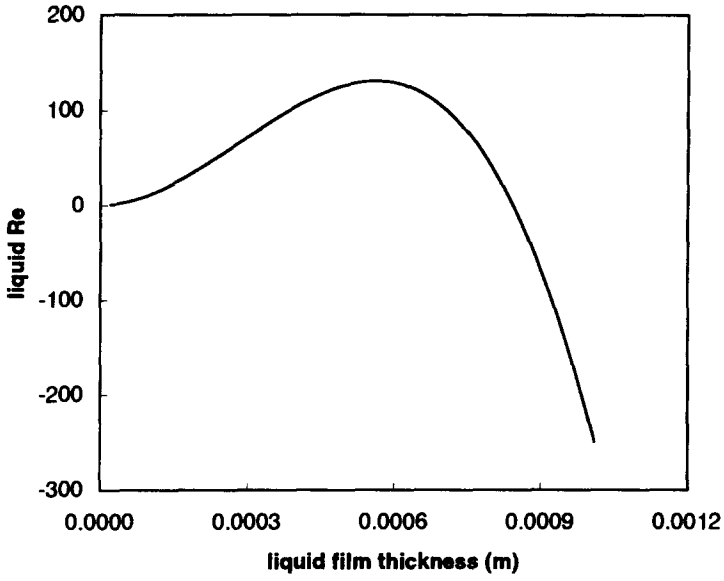

Figure 5. Liquid Re number as a function of liquid film thickness for gas spacing $m = 0.005$ m and pressure drop $\Delta P/L = 500$ N/m^3.

The common conclusion, at the Stokes limit, is that the free surface (or interface) waves have an amplitude that is always smaller than that of the wall corrugations.

In a recent work (Bontozoglou & Papapolymerou 1996), it has been demonstrated that—by relaxing the Stokes flow assumption—a resonance interaction is calculated, leading to stationary surface waves with amplitude larger than the wall. The wavelengths of interest for free falling films are of the order of millimeters, and maximum amplification (wave amplitude/wall amplitude) is around 2.5. As a verification of the validity of the present code, these last results are recovered in the limit of flow driven only by gravity ($\Delta P/L = 0$).

The inclusion of a gas flow turns out to provide more than a trivial extension of previous behaviour. It is intuitively expected that energy input from air to water may enhance interfacial instabilities. Indeed, practically infinite amplifications are calculated from the linear formulation of the present work. Furthermore, an entire series of resonances appears when varying the flow rates. The overall behaviour is very rich and unexpected and—given the large number of independent parameters—particularly difficult to classify in a systematic way.

4.1. Results for low pressure drop

Results are computed for a representative dynamic pressure drop $\Delta P/L = 30$ N/m^3. Infinitesimal corrugations with wavelength L in the range 0.001–0.01 m are considered on a wall at $\phi = 60°$ to the vertical. For each wavelength, the liquid film thickness is the independent parameter. The constant pressure drop chosen is low in the sense that the liquid flow is weakly influenced by the countercurrent gas flow. The velocity profile (a) in figure 2 is representative of the present conditions.

The spacing m (from interface to the zero-stress plane in the gas flow) is kept constant in all runs and equal to 0.005 m. This means that, for the higher liquid flow rates, the overall channel width changes slightly from run to run. The reason behind this choice is to keep Re_G roughly constant, and thus, decrease by one the number of independent parameters. The aforementioned pressure drop and channel dimension correspond to Re_G roughly equal to 100.

The amplitude of the stationary interfacial wave as a function of liquid film thickness is shown—for three representative wavelengths—in figure 3(a)–(c). Two resonance peaks appear in all cases, with the spacing between them decreasing with increasing wall wavelength. This is contrasted with the single resonance, computed (Bontozoglou & Papapolymerou 1996) for a liquid falling film with no air flow.

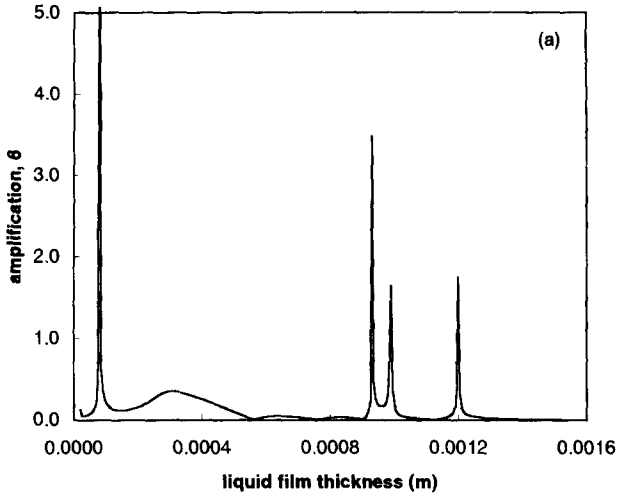
(a)
amplification, β
5.0
4.0
3.0
2.0
1.0
0.0
0.0000
0.0004
0.0008
0.0012
0.0016
liquid film thickness (m)

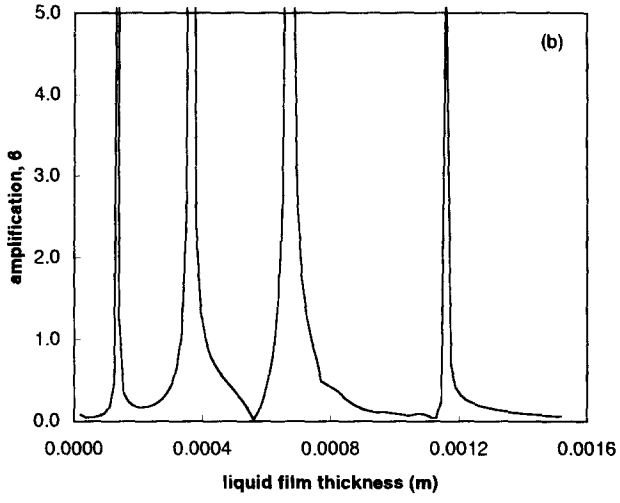
(b)
amplification, β
5.0
4.0
3.0
2.0
1.0
0.0
0.0000
0.0004
0.0008
0.0012
0.0016
liquid film thickness (m)

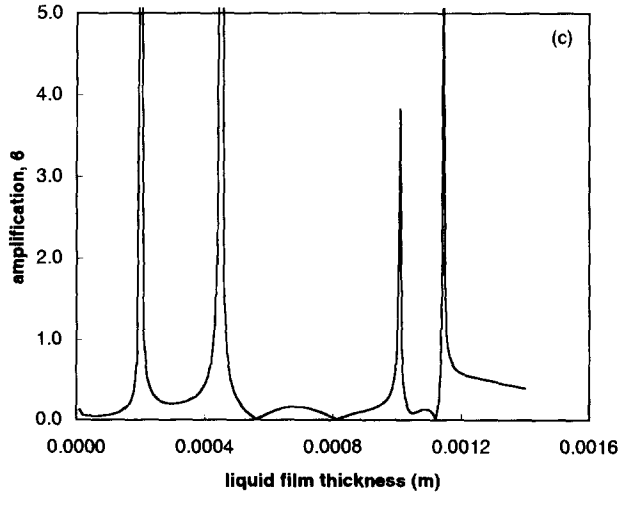
(c)
amplification, β
5.0
4.0
3.0
2.0
1.0
0.0
0.0000
0.0004
0.0008
0.0012
0.0016
liquid film thickness (m)

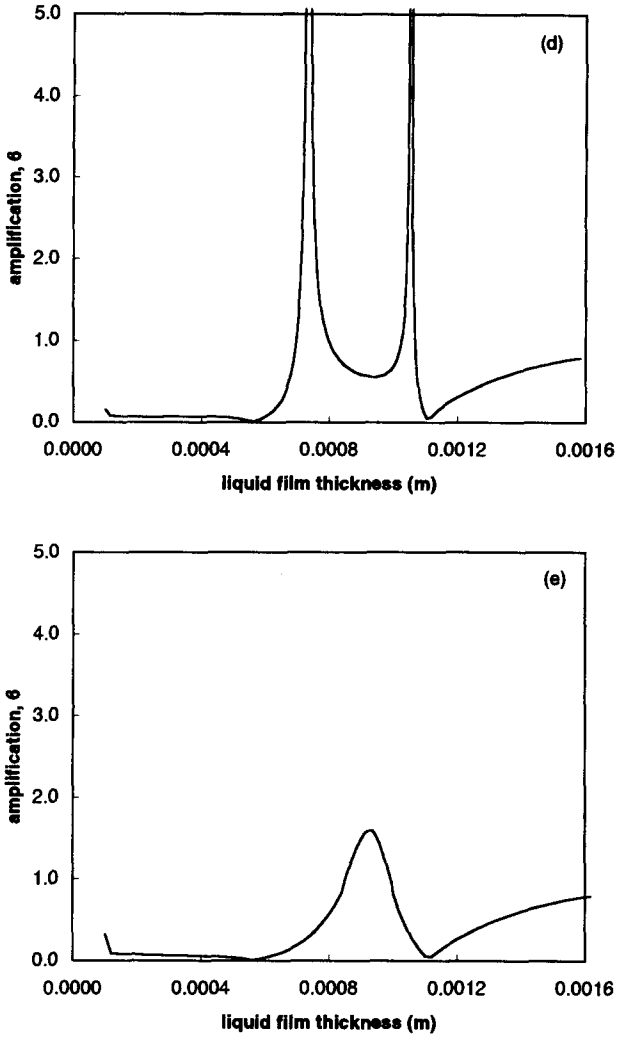

Figure 6. The interfacial amplification as a function of liquid film thickness for gas spacing $m = 0.005$ m and pressure drop $\Delta P/L = 500$ N/m^3. Plots refer to wall corrugations with the following length: (a) 0.0025 m, (b) 0.005 m, (c) 0.001 m, (d) 0.10 m, (3) 0.15 m.

The most important observation is that the two maxima of interfacial amplitude, computed for $L = 0.005$ m and h around 0.00012 and 0.00030 m respectively (figure 3(b)), are practically infinite. Linearly infinite values imply a strong resonance and it is interesting that this result occurs in spite of the dumping effect of viscosity which is rigorously accounted for in the present computation.

Infinite amplification should not be taken literally, since for interfacial waves beyond a certain steepness the linear approximation ceases to be valid. In similar cases (Miles 1986) non-linear theory indicates that the locus of steady solutions becomes triple-valued around the resonance, with two turning points and an unstable middle branch. The value of the present computation lies in the demonstration that genuine resonance—rather than small amplification—takes place at the specific conditions. This behaviour is contrasted with the aforementioned results of the authors for free falling films and is evidently attributed to the effect of gas flow.

Figure 3(a) and (c) demonstrates that, when moving away from exact resonance, the interface amplitude becomes finite and eventually diminishes. As far as parametric dependence on wavelength is concerned, comparison with the falling film results (Bontozoglou & Papapolymerou 1996) indicates that the inclusion of gas flow leads to maximum resonance for longer wall corrugations. Also, the range of wavelengths with strong amplification becomes wider. Results to follow will show that these trends continue with increasing gas velocity.

The interfacial resonance phenomenon can be attributed to a forcing mechanism. The argument is that large stationary waves appear along the interface when the surface velocity of the liquid film becomes equal to the natural phase velocity of interfacial waves at the pertinent flow conditions. Under these circumstances, the wall disturbances can feed energy directly to the interfacial structures. The appearence of two peaks in figure 3(b) can then be justified by the above mechanism. It is well-known that free surface waves have a single solution branch (phase velocity as a function of wavelength), whereas interfacial waves with gas flow have two solution branches (see for example Yih (1979)). Thus, one is led to expect one peak in the falling film computation and two peaks in the gas–liquid flow.

Finally, the phase of the interface relative to the wall roughness is shown (for $L = 0.005$ and $L = 0.0025$) in figure 4(a) and (b). It is interesting that a discontinuous jump is calculated only for one of the resonances (a different one in each case). The other resonance seems to be associated only with a change of curvature in the phase vs film thickness plot.

4.2. Results for high pressure drop

Next, results are presented for a representative dynamic pressure drop $\Delta P/L = 500\ \mathrm{N/m^3}$. Infinitesimal corrugations with wavelength L in the range 0.002–0.2 m are considered on a wall at $\phi = 60^\circ$ to the vertical. The spacing m (from interface to the zero-stress plane in the gas flow) is kept constant in all runs and equal to 0.005 m. The aforementioned pressure drop and channel dimension correspond to $\mathrm{Re_G}$ roughly equal to 2100.

The constant pressure drop chosen is high in the sense that the mean liquid flow changes direction with increasing liquid film thickness. This is demonstrated in figure 5, where $\mathrm{Re_L}$ is seen to start at positive values (in our sign convention this means upward flow, cocurrent with the gas), reach a maximum and then decrease continuously, turning beyond a point to countercurrent flow. This behaviour corresponds to the trivial result that, for high-speed gas flow with constant gas spacing, thin liquid films are conveyed upward by the interfacial drag, whereas thicker films are pulled down by gravity.

The amplitude of the stationary, interfacial wave as a function of liquid film thickness is shown—for five representative wavelengths—in figure 6(a)–(e). A series of four peaks is observed when varying the liquid film thickness over short corrugations. The series degenerates to two peaks for longer wall corrugations. The amplification ratios are practically infinite for wavelengths ranging from 0.005 to 0.1 m, and decrease for longer and shorter waves. The range of liquid film thickness over which resonant phenomena occur is between 0.1 and 1.2 mm.

In comparison to the low gas velocity data, there is an impressive expansion of the parameter space where resonance occurs. Wavelengths triggering infinite amplification now extend over more than an order of magnitude. The expansion is towards longer waves, thus supporting the previous observation of increasing dependence of the most active wavelength on gas velocity.

The appearance of four peaks for short wall disturbances is arguably attributed to the non-uniqueness of the base flow. Indeed, we have two different values of base film thickness for the same $\mathrm{Re_L}$, one corresponding to countercurrent and the other to cocurrent flow. Therefore, the four peaks are two pairs, each associated with the different flow orientation.

5. CONCLUDING REMARKS

Stratified, laminar flow of a liquid and a gas in a channel with corrugated lower wall is considered. An analysis is performed, valid for small-amplitude disturbances but arbitrary wavelength and Re number. Very strong amplification of the wall corrugations at the interface is calculated under certain conditions. The steep variation of amplification ratio with liquid flow rate points to a resonance phenomenon and a tentative mechanism is suggested.

The effect of gas flow is profound. In the two typical cases considered (representative of low- and high-pressure drop) of thin-film flow in a channel with inclination, the amplification at exact resonance becomes linearly infinite. With increasing gas velocity, the range of corrugation wavelengths most active in producing strong interaction with the interface expands considerably, and moves to higher values.

The present study demonstrates a qualitative difference between gas–liquid and free-falling film flows. Indeed, previous results concerning the later indicated only linearly finite amplification. It can be conjectured that the resonant phenomenon under consideration will influence the interfacial dynamics of gas–liquid flows in small-scale passages. Testing of this computational prediction could provide motivation for experimental work on two-phase flow over wavy surfaces, which seems to be presently lacking.

Acknowledgements—The help of Dr Providas (of the Department's Laboratory of Digital Computing) with the installation and operation of a workstation is deeply appreciated.

REFERENCES

Bontozoglou, V., Kalliadasis, S. and Karabelas, A. J. (1991) Inviscid free-surface flow over a periodic wall. *J. Fluid Mech.* **226,** 189–203.

Bontozoglou, V. and Papapolymerou, G. (1997) Laminar film flow down a wavy incline. *Int. J. Multiphase Flow* **23,** 69–79.

Dassori, C. G., Deiber, J. A. and Cassano, A. E. (1984) Slow two-phase flow through a sinusoidal channel. *Int. J. Multiphase Flow* **10,** 181–193.

Hanratty, T. J. (1983) Interfacial instabilities caused by air flow over a thin liquid layer. In *Waves on Fluid Interfaces*, ed. E. R. Meyer. Academic Press, New York, pp. 221–259.

Kennedy, J. F. (1963) The mechanics of dunes and anti-dunes in erodible-bed channels. *J. Fluid Mech.* **16,** 521–544.

Mei, C. C. (1969) Steady free surface flow over a wavy bed. *J. Eng. Mech. Div. ASCE* **EM6,** 1393–1402.

Miles, J. W. (1986) Weakly non-linear Kelvin–Helmholtz waves. *J. Fluid Mech.* **172,** 513–529.

Pozrikidis, C. (1988) The flow of a liquid film along a periodic wall. *J. Fluid Mech.* **188,** 275–300.

Sammarco, P., Mei, C. C. and Trulsen, K. (1994) Non-linear resonance of free surface waves in a current over a sinusoidal bottom: a numerical study. *J. Fluid Mech.* **279,** 377–405.

Wang, C.-Y. (1981) Liquid film flowing slowly down a wavy incline. *AIChE J.* **27**(2), 207–212.

Yih, C.-S. (1979) *Fluid Mechanics*. West River Press, Ann Arbor.